Clinical Radiology xxx (xxxx) xxx

Contents lists available at ScienceDirect

Clinical Radiology

journal homepage: www.clinicalradiologyonline.net

Review

The emerging applications of cardiovascular magnetic resonance imaging in transcatheter aortic valve implantation

C. Mahon [a], R.H. Mohiaddin [a,b,*]

[a] Royal Brompton and Harefield NHS Foundation Trust, London, UK
[b] National Heart and Lung Institute, Imperial College London, London, UK

ARTICLE INFORMATION

Article history:
Received 10 September 2019
Accepted 13 November 2019

Transcatheter aortic valve implantation (TAVI) is an alternative to surgical aortic valve replacement in selected patients with severe symptomatic aortic stenosis (AS) and high surgical risk. The planning and follow-up of TAVI requires an array of imaging techniques, each has advantages and limitations. Echocardiography and multidetector computer tomography (MDCT) have established applications in patient selection and procedure guidance, but are limited in some patients. TAVI applications of cardiovascular magnetic resonance imaging (CMRI) are emerging. CMRI can provide the structural and functional imaging details required for TAVI procedure in away comparable or superior to that obtained by echocardiography and MDCT combined. In this review, we look at the continuously evolving role of CMRI as a complimentary or an alternative to more established imaging techniques and address the advantages and disadvantages of CMRI in this setting. We discuss the role of CMRI in selecting anatomically suitable patients for the TAVI procedure and in the post-TAVI follow-up with particular emphasis on its applications for assessing AS severity and haemodynamic impact, vascular imaging for TAVI access route, quantification of paravalvular leaks and LV remodelling in the post TAVI setting as well as providing imaging biomarkers tool for AS risk-stratification.

Introduction

Degenerative aortic stenosis (AS) is the most common valvular heart disease of the western world.[1] In general, AS is a condition of the elderly carrying a poor prognosis following the onset of symptoms. The prevalence of AS is 3% in those >75 years of age,[2] and is expected only to rise with an aging population.[3] AS intervention is indicated following symptom onset and when there is an anticipated improvement in quality of life or survival. For many years, surgical aortic valve replacement (SAVR) was the reference standard of treatment; however, in an ageing, multimorbid and high-risk population a significant number were declined SAVR. A demand grew for an alternative and less invasive therapy. The alternative was found in transcatheter aortic valve insertion (TAVI). Since its introduction in 2002, TAVI has proved its value as a replacement to SAVR in high-risk inoperable AS patients.[4,5] Its growing authority in the management of high-risk AS patients is acknowledged in the most recent European guidelines on valvular heart disease[3] particularly when transfemoral access is possible.

* Guarantor and correspondent: R. H. Mohiaddin, Royal Brompton Hospital, Sydney Street, London, SW3 6NP, UK.
E-mail addresses: r.mohiaddin@rbht.nhs.uk, r.mohiaddin@imperial.ac.uk (R.H. Mohiaddin).

https://doi.org/10.1016/j.crad.2019.11.011
0009-9260/

Please cite this article as: Mahon C, Mohiaddin RH, The emerging applications of cardiovascular magnetic resonance imaging in transcatheter aortic valve implantation, Clinical Radiology, https://doi.org/10.1016/j.crad.2019.11.011

Not only do the guidelines reflect the evolving role of TAVI in AS, it also addresses the technical and anatomical risk profiles to be considered by the multidisciplinary team in therapy selection. More recently, TAVI has demonstrated promise as an alternative to SAVR in intermediate-risk patients,[6] valve-in-valve treatment for failing bioprosthesis, treatment of bicuspid valves in younger patients with complex anatomical features, and for native pure aortic regurgitation.[7]

Selection of anatomically suitable patients for TAVI

After criteria of severe symptomatic AS and high surgical risk are determined, the technical evaluation of suitability for the percutaneous implantation needs to be assessed including implant sizing and vascular appraisal. Appropriate sizing of the valve is crucial to reduce the incidence of paravalvular leak, conduction disturbance, functional stenosis, or life-threatening complications, such as valve embolisation or annular rupture. There are three main types of TAVI implant mechanisms on the market including the balloon-expandable, the self-expandable, and the mechanically expandable implants (Table 1). Valve sizing is based on one or more annular measurements including perimeter, diameter, and/or area. The optimal choice of annular measurement is based on the valve type and charts are available to optimise choice. Minimal distance of the annulus to the coronary ostia, size of the sinus, and degree of calcification are important parameters also to avoid coronary occlusion. Ribeiro and colleagues demonstrated that a lower-lying coronary ostium (<12 mm) and shallow sinuses of Valsalva (<30 mm) were the strongest anatomical factors associated with coronary obstruction.[8] Because of the relative large delivery systems, careful evaluation of the access vessels and the route to the AV is also needed to avoid vascular and neurological complications. A virtual roadmap of the vessels is therefore acquired prior to TAVI. The preferred access is the ilio-femoral vessels, although subclavian, carotid, and transapical are alternative options. Imaging plays a vital role in all aspects of this assessment.

Imaging methods

The planning for a TAVI procedure requires an array of imaging techniques (Table 2), designed not only to select an appropriately sized implant, but also to identify the potential obstacles to procedural success.[9] In recent years echocardiography along with multidetector computer tomography (MDCT) have formed the cornerstone of imaging in patient selection and procedure guidance for TAVI.[4,5] Cardiovascular magnetic resonance imaging (CMRI) is reserved as an alternative to MDCT and/or echocardiography in select patients; in particular, when there is a poor renal function or other contraindication to MDCT iodinated contrast agent, or in patients with poor echocardiographic images or discrepant results[4,5]; however, the role of CMRI in TAVI assessment is likely to change in the future. Not only as a potential replacement for MDCT, but current research is focusing on identifying risk-stratification tools for earlier intervention in this high-risk AS population including assessment of the LV remodelling and fibrosis. This article focuses on the current clinical application and the evolving role of CMRI in AS and TAVI.

Echocardiography

Transthoracic echocardiography (TTE) remains the standard technique in the assessment of AS severity, progression, and prognosis[3] using the continuity equation. In addition, it also evaluates left and right ventricular function, wall thickness, and valvulopathy. It is a relatively cheap imaging technique, well tolerated by the elderly, and is widely available; however, identifying low-flow low-gradient severe AS is a technical challenge with TTE, and it is limited in accurately measuring annular and sinus dimensions for TAVI. Low-dose dobutamine stress TTE can aid in identifying low-flow low-gradient AS. Three-dimensional (3D) TTE or transoesophageal echocardiography (TOE) can provide more accurate annular and root measurements compared to conventional TTE; however, TOE is a semi-invasive technique and poorly tolerated in the elderly. Up until recently, intra-procedural TOE did also play a key role in monitoring TAVI procedures. TOE was used to detect complications such as paravalvular leak, mitral valve damage, pericardial effusion, ventricular function, and aortic rupture or dissection before and after balloon aortic valvuloplasty[10]; however, the TAVI procedure is increasingly being performed under conscious sedation, and the role of intra-procedural TOE has declined. TOE is now reserved for select patients. One interesting role for TOE-guided TAVI lies in EchoNavigator technology providing fusion imaging of

Table 1
The main commercially available transcatheter valve implants and their valve structure.

Implant name	Valve structure
Sapien 3 (Edwards Lifesciences)	Bovine pericardial tissue valve; balloon-expandable cobalt chromium frame
Evolut R (Medtronic)	Porcine pericardial tissue valve; self-expanding nitinol frame
Portico (St Jude Medical, Inc.)	Bovine pericardial tissue valve; self-expandable nitinol alloy stent
Accurate Neo (Symetis)	Porcine pericardial tissue valve; self-expandable nitinol alloy stent
JenaValve (JenaValve Technology GmbH)	Porcine pericardial tissue valve; self-expanding nitinol stent
Lotus (Boston Scientific Corporation)	Bovine pericardial tissue valve; self-expanding, braided nitinol frame
Allegra (NVT AG)	Bovine pericardial tissue valve; self-expanding nitinol stent

Please cite this article as: Mahon C, Mohiaddin RH, The emerging applications of cardiovascular magnetic resonance imaging in transcatheter aortic valve implantation, Clinical Radiology, https://doi.org/10.1016/j.crad.2019.11.011

Table 2
Commonly used imaging methods for transcatheter aortic valve insertion work-up and relative advantages and disadvantages.

	Role	Advantage	Disadvantage
Transthoracic echocardiogram	Measures peak aortic valve velocity, gradients, valve area, and overall cardiac function Assess prosthetic valve function; qualitatively and semi-quantitatively assess severity of paravalvular aortic regurgitation	Can be performed at the bedside Non-invasive No nephrotoxic contrast Non-radiation Cheap, portable and widely available	Low-dose dobutamine stress required if suspected low-flow low-gradient aortic stenosis Poor acoustic windows may limit study
Transoesophageal echocardiography	Measures aortic annulus and root, coronary artery ostial height	Intra-procedural monitoring	Semi-invasive
Cardiac computed tomography	Measures dimensions of aorta, annulus, root, coronary ostial height, peripheral vasculature assessment Assess location and severity of aortic valve and ascending aortic calcification Determine optimal valve implantation projection angles Determine access route suitability Investigate suspected vascular access complications	Visualisation of aortic root calcification Relatively short scan time Non-invasive	Nephrotoxic contrast agent Radiation exposure Cannot be performed at the bedside Calcification artefact may preclude accurate ileo-femoral luminal measurement
X-ray fluoroscopy	Define coronary artery anatomy and severity of disease Guide valve implantation Measure right and left pulmonary artery pressures	Procedural guidance	Invasive Cost Radiation Nephrotoxic agent
Cardiac magnetic resonance imaging (MRI)	Measures aortic valve velocity, valve area, and overall cardiac function Measures dimensions of aorta, annulus, root, coronary ostial height, peripheral vasculature assessment. Determine optimal valve implantation projection angles Assess vascular complications Assess prosthetic valve function; qualitatively and semi-quantitatively assess severity of paravalvular aortic regurgitation Quantify diffuse myocardial fibrosis	Non-invasive No nephrotoxic contrast Non-radiation Quantifies myocardial fibrosis and focal scar Quantification of transvalvular and paravalvular regurgitation Assess for TAVI procedure-related myocardial injury	Suboptimal visualisation of calcification Long duration of acquisition High cost and limited availability MRI non-compatible device

TOE and fluoroscopy in real time.[9] This optimises implant deployment position, and potentially allows for zero contrast TAVI procedures, which can be advantageous in patients with renal impairment.[9] Importantly the shift away from TOE-guided TAVI, according to one French registry, has not impacted on outcomes.[11] TTE is currently used after TAVI implantation to detect implant position and complications. It is further used in the long-term follow-up of TAVI patients to monitor the valve function.

MDCT

MDCT is the preferred imaging technique to provide information beyond AS severity for TAVI work-up. It provides information on the number of AV cusps, aortic root assessment, annulus size, ostial height, and degree of calcification, all of which are important for prosthesis sizing.[12] MDCT looks at the feasibility of various access routes, and provides vascular information on the minimal luminal diameters, atherosclerotic burden, calcification, aneurysms, tortuosity, and aortic root measurements. In addition, automatic software enables an accurate prediction of implantation angles for the TAVI procedure.[13] Overall, offering a virtual roadmap of the vasculature to identify potential obstacle during the procedure. Such information allows the planning of access routes with a view to minimising vascular complications. This greatly improves the success of TAVI, where the rate of complications related to vascular access has been reported as anything between 6.3 and 30.7%.[14] In select patients with a low risk of coronary artery disease, MDCT can avoid the need for invasive coronary angiography pre-TAVI; however, at present, there are still technical limitations in coronary artery assessment with MDCT, particularly in severe and calcific coronary artery disease.[9]

CMRI

In recent decades, CMRI has emerged as complimentary or alternative imaging technique to TTE and MDCT for assessment of AS, TAVI planning and post-TAVI follow-up. This is particularly true in patients with poor acoustic TTE

Please cite this article as: Mahon C, Mohiaddin RH, The emerging applications of cardiovascular magnetic resonance imaging in transcatheter aortic valve implantation, Clinical Radiology, https://doi.org/10.1016/j.crad.2019.11.011

Table 3
Classification of the severity of aortic stenosis, based in part on the 2006 ACC/AHA Guidelines.[16]

	Mild	Moderate	Severe
Peak jet velocity (m/sec)	<3	3–4	>4
Orifice area (cm^2)	>1.5	1.0–1.5	<1.1
Orifice area index (cm^2/m^2)			<0.6
Additional features			Left ventricle hypertrophy, post-stenotic dilation of the ascending aorta

images because CMRI offers unlimited windows. In patients with renal failure and other contraindications to iodinated contrast agent it offers a non-contrast or non-nephrotoxic contrast-enhanced vascular imaging alternative to MDCT.

Like echocardiography, CMRI can provide information on AV anatomy, quantifying stenosis, overall cardiac structure, and function with high accuracy. It is the reference standard for assessment of ventricular volumes, mass and function.[15,16] It is the method of choice when there are conflicting findings in complex AV disease, such as stenosis at more than one level or where there is ambiguity over the severity of AS. Table 3 lists the range of measurements reflecting different severities of AS.[17] It offers insight into the role of LV remodelling in the setting of severe AS, to detect myocardial fibrosis, and evidence of coronary artery disease.[18] This multiparametric comprehensive assessment for tissue characterisation of the myocardium is the focus of research aiming to risk-stratify patients for earlier intervention with the ultimate role of improving outcomes.[19]

CMRI can also provide similar information provided by MDCT. In single-centre studies, excellent correlation has been demonstrated between CMRI and MDCT in assessment of ostial height, annular, and aortic root dimensions.[20] These measurements usually made in diastole, but can be obtained in systole if systolic assessment is required.[21,22] It provides information on the feasibility of the various access routes and aortic information paramount to procedural success including lumen diameters, atherosclerotic burden, and identifies vessel anomalies. TAVI is increasingly being used in younger and intermediate-risk patients and cardiac MRI offers a radiation free diagnostic assessment for these patients.

CMRI does have its own limitations. The available access to CMRI and cost limits its use in different health services.[23] It requires greater cooperation by patients to remain still and in breath-holding sequences. Both of which can lead to artefact, although technical developments are decreasing scan time with faster imaging sequences and free-breathing sequences. In addition to motion and respiratory artefacts, there are other artefacts including metal artefact and chemical shift. The TAVI implant is MRI compatible and generates only minimal artefact (Fig 1). This review does not describe the artefacts in detail, but they are worth mentioning and more information on the recognition and management of artefacts can be found elsewhere by the interested reader.[24]

CMRI is less sensitive in the evaluation of calcification compared to MDCT. A noteworthy limitation given that calcium quantification and distribution has been associated with TAVI complications including paravalvular leak and pacemaker insertion.[25,26] Temporal resolution (the precision of a measurement with respect to time) is inferior to echocardiography, making it difficult to access small fast moving structures. (Note: spatial resolution is the number of pixels used in construction of a digital image.) AV velocities are prone to being underestimated compared to echocardiography if the imaging plane is positioned too far downstream of the AS stenotic jet.[27,28] Various implanted devices, including pacemakers, are occasionally both a relative and absolute contraindication to CMRI. Gadolinium-based contrast agents (GBCAs) have been linked to nephrogenic systemic fibrosis (NSF) resulting from slow renal excretion and dissociation of gadolinium.[29] The incidence NSF has reduced dramatically since 2009 owing to the restrictions on linear-based agents, the switch to macrocyclic agent (e.g., gadobutrol) and renal function check. No new cases related to exposure to the agents following the restrictions have been reported in Europe.[30] More recently, a series of publications investigating signal hyperintensity on unenhanced T1-weighted MRI of the brain in patients administered multiple doses of gadolinium

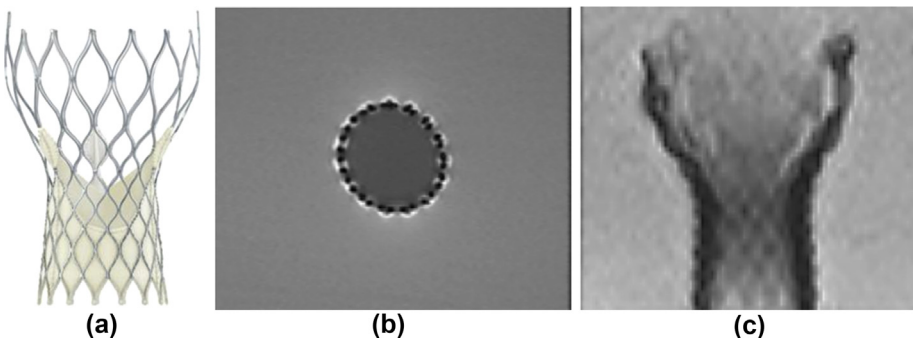

Figure 1 (a) Medtronic Corevalve, ex-vivo bSSFP MRI of the transcatheter aortic valve (b,c) suspended in water doped with copper sulphate depicting the metal skeleton (Nitinol) of the valve.

Please cite this article as: Mahon C, Mohiaddin RH, The emerging applications of cardiovascular magnetic resonance imaging in transcatheter aortic valve implantation, Clinical Radiology, https://doi.org/10.1016/j.crad.2019.11.011

indicate that there may be long-term gadolinium retention in the brain.[31,32] The sequela, if any, remains to be determined.

Indications and protocol for CMRI TAVI

TTE and MDCT are the current key diagnostic tests for TAVI work-up. CMRI can provide equivalent information offered by both methods required for AS assessment and TAVI work-up. To obtain this information, specific CMRI sequences are tailored to produce anatomical, structural, and functional imaging. Sequences differ depending on the information required. Balanced steady state free precession (bSSFP) cine sequences, phase contrast sequences, T1-and T2-weighted fast spin-echo (FSE) sequences, T1 mapping, myocardial gadolinium-enhancement sequences along with 3D SSFP, are the most widely used. A gradient echo sequence (fast low angle shot [FLASH]) is an alternative sequence for functional assessment if the valve-related metal artefact is significant. Cardiac specific sequences are typically implemented on 1.5 T MRI systems. A proposed standard protocol in TAVI work-up is depicted in Table 4. In brief, the protocol includes: (1) an anatomical assessment of the neck to femoral region by acquiring transaxial bSSFP black-blood FSE images of the region of interest. Coronal and sagittal orientations can also be acquired; (2) ventricular volumes, function, and mass are assessed using high spatial resolution bSSFP cine sequences taken in three long axis views (two-chamber, four-chamber and left ventricular outflow tract [LVOT]) and in a short axis stack from the atrioventricular valves through to the apex; (3) severity of AS is determined from AV area using planimetry and maximum gradients using phase contrast (PC) velocity mapping. Planimetry also allows for assessment of the sinus, annulus, and LVOT. Planimetry images are acquired using a bSSFP short axis stack cine sequences from upstream to downstream of the AV valve. The maximum velocity requires PC velocity-encoding cines at the level of the sino-tubular junction and the AV; (4) aortic assessment of dimensions, atheroma, tortuosity, and other aortic pathology is determined using an oblique bSSFP cine of the aorta and an oblique sagittal, transaxial, and coronal half-Fourier acquisition single-shot turbo spin-echo (HASTE); (5) myocardial characterisation requires a T1 mapping sequence using the modified look-locker imaging sequence (MOLLI), and gadolinium images. Early gadolinium can identify thrombi, and late gadolinium enhancement (LGE) myocardial imaging should be acquired in the same views as previously acquired for myocardial cine sequences; (6) A vascular roadmap to provide information on access routes, ostial height and procedural obstacles is obtained through a 3D free-breathing SSFP to include the ileofemoral vessels, aorta, aortic root, carotids, subclavian vessels, and at times, the circle of Willis.

Table 4
Proposed cardiac magnetic resonance imaging protocol for transcatheter aortic valve insertion work-up.

Cardiac Anatomy	5 min
Ventricular function Two-, four-, and three-chamber Short-axis bSSFP cine images of the ventricles	10 min
Aortic valve assessment Short-axis bSSFP cine of the AV	10 min
Flow mapping Phase contrast velocity mapping	5 min
Aorta Oblique sagittal, transaxial HASTE images	5 min
T1 mapping Modified look-locker imaging sequence	5 min
Vascular Roadmap Three-dimensional bSSFP, consider CE-MRA	5 min
Myocardial LGE Same views	5 min

bSSFP, Balanced steady state free precession; HASTE, half-Fourier acquisition single-shot turbo spin-echo; CE-MRA.

Measurement of ventricular volumes and function

CMRI is the reference standard for assessment of ventricular volumes, mass, and function,[16] with lower intra- and interobserver variability than echocardiography.[33] Normal reference LV and right ventricular (RV) values are available.[34] LV volumes can be deleteriously impacted by pressure overload secondary to AS, and offer prognostic information prior to TAVI. Conversely, post-TAVI remodelling can demonstrate improvement in ventricular volumes, mass, and function.[35]

The typical approach involves conventional breath-holding bSSFP cine images, or free-breathing gradient echo sequences. These are acquired in the two-, three- and four-chamber long axis views. These long axis views are then utilised to plan a short-axis stack from the mitral annulus to apex. Recent developments allow real-time bSSFP images to be obtained in a single breath-hold.[36] This is advantageous in patients that are unable to hold their breath for significant periods or patients with orthopnoea. Off-line analysis using commercially software is used to determine volumes, function, and mass employing the summation of disks method (Fig 2).[37] Simpson's Rule is a fourth-order polynomial approximation of numerical integration. The mathematical and clinical definition differ somewhat. The term "modified Simpson's Rule" has been coined by echocardiography to refer to a simplified summation of disk method. With the summation of disk method, the cross-sectional area in each short axis section is measured, multiplied by the section thickness (and any intersection gap if applicable), and summed over the entire

Please cite this article as: Mahon C, Mohiaddin RH, The emerging applications of cardiovascular magnetic resonance imaging in transcatheter aortic valve implantation, Clinical Radiology, https://doi.org/10.1016/j.crad.2019.11.011

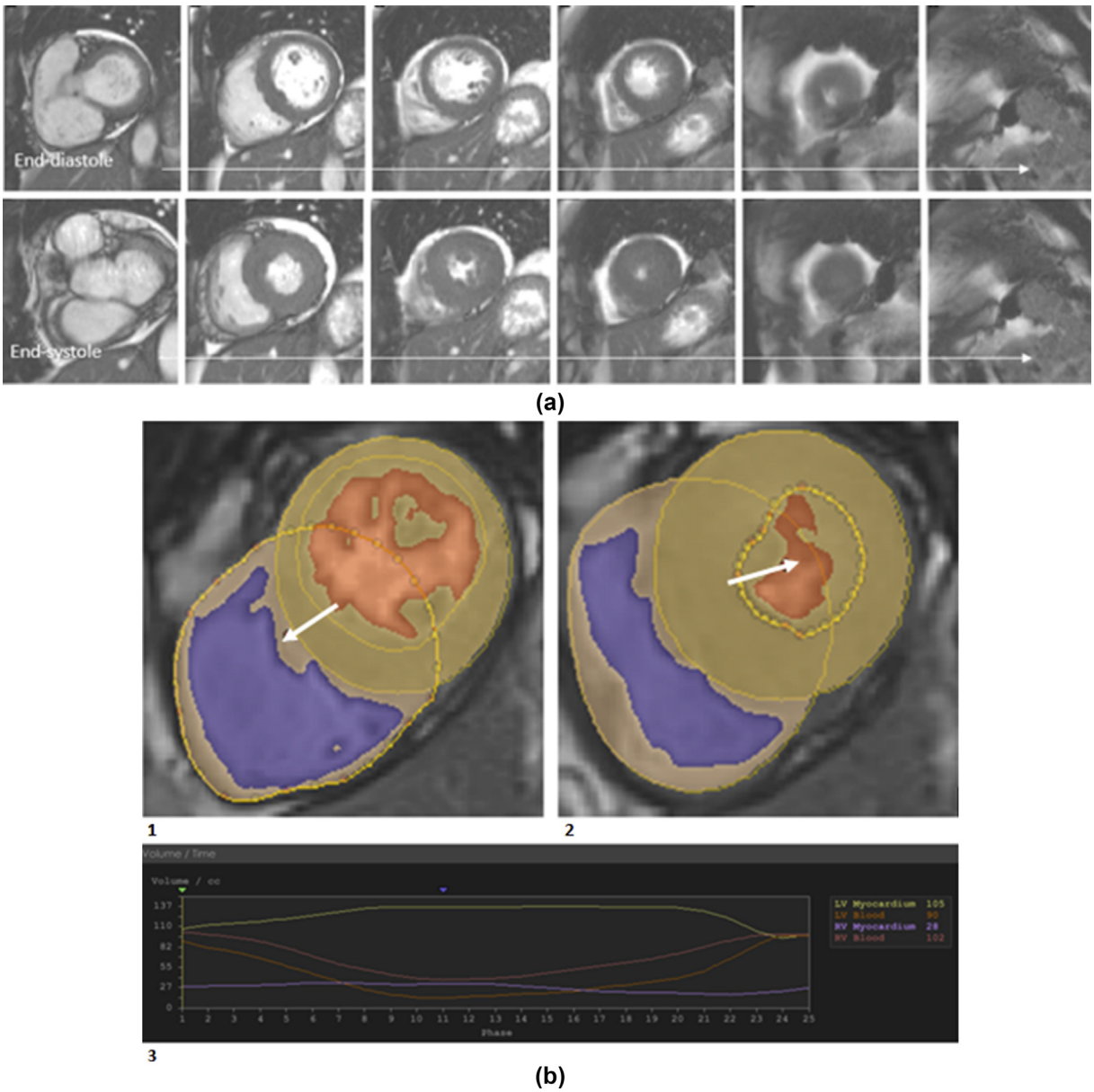

Figure 2 (a) Selected images from the complete cine bSSFP acquisitions in the ventricular short axis view from base to apex in end-diastole (upper panel); and the corresponding slices in end-systole (lower panel). (b) To determine the ventricular volumes, function, and mass the LV epicardial, left endocardial, and right endocardial surfaces are semi-automatically segmented from bSSFP images in end-diastole (1); end-systole (2) using CMRtool software; and volume–time curve of ventricular volumes for a cardiac cycle (3). Arrows demonstrate the right (1), and left (2) ventricle, respectively.

LV.[37,38] Regional LV systolic function can be assessed both qualitatively and quantitatively. This can be mapped onto the 17-segment American Heart Association Model for qualitative assessment of wall thickening.[39] A similar method is used for RV assessment.

Measurement of ventricular myocardial mass

Pressure overload secondary to severe AS is associated with LV remodelling, in-particular LV hypertrophy. The Framingham Study showed that increases in LV mass are associated with increased cardiovascular morbidity and mortality independent of coronary artery disease or other cardiovascular risk factors.[40,41] Electrocardiographic criteria for LV hypertrophy have been in use for several decades.[42,43] These criteria were mostly validated against M-mode TTE[44] and lacked the sensitivity for LV hypertrophy. They have recently been recalibrated against CMRI and this has improved diagnostic accuracy.[45] CMRI gives a precise measurement of LV wall thickness.[46] Using LV mass assessment and LV wall thickness any degree of LV hypertrophy can be assessed.[47] The mass of the LV wall can be

Please cite this article as: Mahon C, Mohiaddin RH, The emerging applications of cardiovascular magnetic resonance imaging in transcatheter aortic valve implantation, Clinical Radiology, https://doi.org/10.1016/j.crad.2019.11.011

estimated by measuring the volume of the myocardium (using the volumetric summation method, described above) and multiplying it by the specific gravity of myocardium, 1.05 g/ml.

CMRI not only quantifies, but also assess the pattern of LV hypertrophy. It provides a good understanding of the LV remodelling in the presence of pressure overload due to AS. There is variation in the remodelling response to AS for similar degrees of severity. CMRI has played a key role in identifying these different patterns of remodelling, ranging from concentric to eccentric hypertrophy prior to dilation and decompensation.[35] Concentric and eccentric hypertrophy can be distinguished using relative wall mass.[48,49] Relative wall mass is calculated by dividing the LV mass by the LV end-diastolic volume, and effectively indexes ventricular wall thickness to cavity size.[50] Increased LV mass with relative wall mass above or below the cut-off value of 1.16 distinguishes concentric from eccentric respectively. Concentric hypertrophy has consistently been shown to be the condition that most markedly increases cardiovascular risk.[51] Importantly, LV hypertrophy of any aetiology confers increased cardiovascular risk, and conversely, regression has been shown to decrease cardiovascular risk.[52] CMRI has already been used to quantify reverse remodelling following intervention.[53] It can be used to determine ventricular mass regression in post-TAVI patients. CMRI has also provided important insights into the gender differences in the remodelling response. Men demonstrate higher indexed LV volumes, LV mass, more concentric remodelling, worse LV systolic, and diastolic function than female patients with a similar degree of AS.[54,55]

Assessment of AS

Planimetry

CMRI images allow for direct visualisation of the AV orifice for morphology and planimetry. AV planimetry by CMRI has very good agreement with TTE[56] and TOE.[57] AV planimetry and the calculated effective orifice area (EOA) using continuity equation are not the same measurement. EOA represents the mean area in systole and can be influenced by flow convergence downstream of the anatomical area, whereas, the AV planimetry represents the maximum instantaneous AV area in systole. Planimetry represents the maximum systolic AV area in systole rather than the mean AV area. Therefore, the thresholds for severity are higher for planimetry as demonstrated using MDCT AV area.[58,59]

Planimetry sequences are obtained from serial short-axis bSSFP cines of the AV valve to form a stack. The stack typically has five sections, shifting 3 mm at a time from immediately upstream to downstream of the orifice. Overlapping sections is an alternate approach (Fig 3). The thin structure of the AV leaflet can be clearly visualised if appropriately aligned. The cine image with the smallest, most clearly delineated cross-section of the orifice should be used for planimetry. A flat jet through a slit-like orifice will be clearly seen if the image plane cuts perpendicular to the line of the slit in a plane aligned with the length of the slit.[60]

Phase-contrast velocity mapping

In addition to valve area planimetry, CMRI can provide reliable measurements of flow and velocity through the stenotic AV, in a similar manner to the Doppler study of TTE. The CMRI technique used is phase-contrast (PC) velocity mapping, which has been validated extensively in the assessment of valvular heart disease.[28,61] The measurements of pressure gradients correlates well with the accepted standard of Doppler ultrasound.[28] In patients with inadequate echocardiographic quality or discrepant results, it is recognised that CMRI should be used to assess the severity.[3] PC is a gradient-echo sequence that uses both the phase and amplitude of the signal to create a velocity map.[62,63] PC imaging can be obtained in plane or through plane (Fig 4). Through-plane PC images are preferred to in-plane PC images for estimation of peak velocity. The velocity encoding (VENC) must be specified before performing a PC

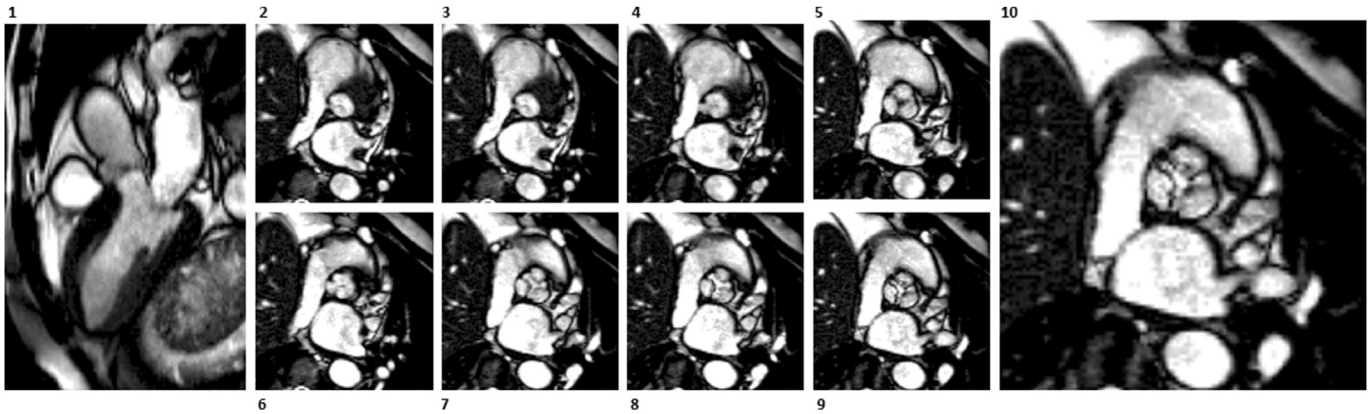

Figure 3 (1) bSSFP image in the LVOT view depicting serial contiguous short-axis bSSFP cine images of the aortic valve to form the stack (each slice is 5 mm in thickness). (2–5) end-diastolic aortic valve stack (each slice is 5 mm in thickness). (6–9) end-systolic aortic valve stack. (10) Magnified selected image for planimetry of the severely stenotic aortic valve.

Please cite this article as: Mahon C, Mohiaddin RH, The emerging applications of cardiovascular magnetic resonance imaging in transcatheter aortic valve implantation, Clinical Radiology, https://doi.org/10.1016/j.crad.2019.11.011

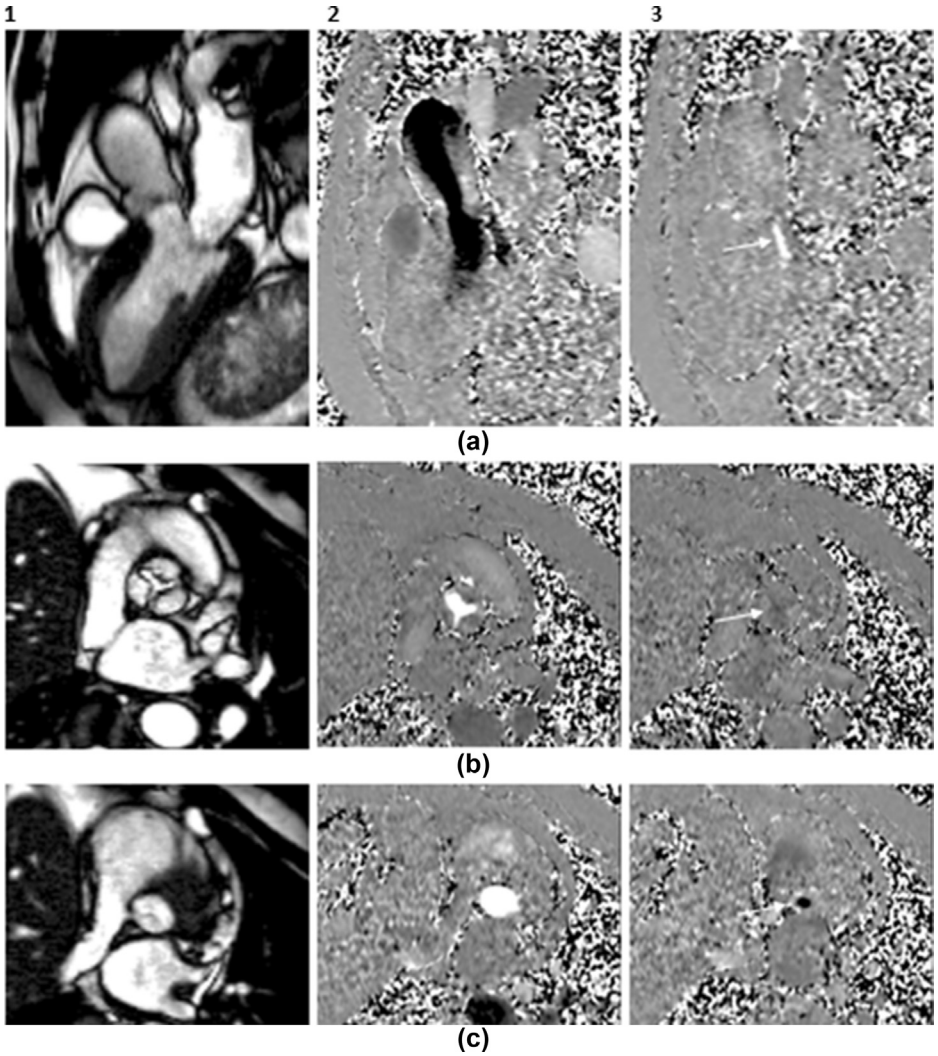

Figure 4 (a) Balanced steady state free precession (bSSFP) anatomical image in the LVOT view and the corresponding in-plane phase contrast (PC) velocity mapping of the aortic valve in systole (1) and diastole (2), depicting the aortic stenotic and regurgitant jet respectively (arrow). (b) bSSFP anatomical image in the AV short axis view and the corresponding through plane PC velocity mapping of the aortic valve (AV) in systole (1) and diastole (2), depicting flow through the severely stenotic aortic valve in systole and regurgitant jet in diastole (arrow). (c) bSSFP anatomical image at aortic annulus level and the corresponding through plane PC velocity mapping in the subaortic valve at systole (1) and diastole (2) depicting the AR jet (arrow).

sequence. VENC is user selected and should be slightly higher than the actual velocity to avoid aliasing. If the selected VENC is too high, then the sensitivity to detect a maximum velocity decreases. Ideally, it should not exceed 20% higher than the actual velocity. Off-line analysis of the through-plane images in all phases of the cardiac cycle derives a velocity aortic flow curve. The curve identifies the maximum velocity and all other parameters of flow (including regurgitant jets). CMRI flow velocities can be underestimated compared to echocardiography Doppler particularly at higher velocities.[27] This is partly because PC measures averaged velocities compared with instantaneous peak velocities measured on Doppler or if the imaging plane is positioned too far downstream of the AS stenotic jet.[63]

Importantly, as the role of TAVI evolves, the aortic flow curves derived from PC images can also be used to quantify aortic regurgitation in patients with mixed native AV disease, valve-in-valve failing bioprosthetic valves and native aortic regurgitation. In the post-procedure setting, CMRI can also accurately access paravalvular leak.[64]

Valve sizing

MDCT is the reference standard for annulus measurements for TAVI sizing. 3D TTE and TOE are the most common alternative techniques used to obtain annulus measurements in patients with severe renal dysfunction or iodinated contrast allergy. Two-dimensional bSSFP cine images and a step-by-step fashion reconstructions of respiratory gated 3D bSSFP non-contrast CMRI acquisition has been described as an alternative to MDCT measurements of valve sizing, without the need for nephrotoxic contrast agent.[65] The method for valve sizing in CMRI is

Please cite this article as: Mahon C, Mohiaddin RH, The emerging applications of cardiovascular magnetic resonance imaging in transcatheter aortic valve implantation, Clinical Radiology, https://doi.org/10.1016/j.crad.2019.11.011

demonstrated in Fig 5. In comparisons of CMRI versus MDCT, in two single-centre studies Pontone *et al.* and Jabbour *et al.* have demonstrated excellent correlation for standard aortic root metrics, which is superior to TTE[20,66] (Fig 6). CMRI may also be used in patients with failing prosthetic valves under investigation for valve-in-valve TAVI, albeit metallic artefact can prevent accurate assessment in certain patients.[67]

Myocardial tissue characterisation

CMRI can characterise the myocardium uniquely and non-invasively using GBCAs (Fig 7). It allows identification of infarcted tissue, quantification of replacement fibrosis, and amyloid. LGE can detect subendocardial infarcted tissue and determine viability in patients with LV dysfunction and coronary artery disease.

Fibrotic burden is a key determinant of both systolic and diastolic LV dysfunction. The correlation of fibrosis and LGE on CMRI has been validated in surgical biopsy studies of AS patients.[18,68] LGE has been shown to be inversely associated with the degree of functional improvement post AVR,[69] and inversely associated with all-cause mortality.[18] In one large multicentre study of patients with severe AS who underwent SAVR or TAVI, fibrosis detected on LGE was present in half the patients and was an independent predictor of mortality post-intervention; its presence was associated with a twofold higher rate of mortality.[70] There is clinical equipoise to determine whether the use of imaging biomarkers of fibrosis can be used to improve outcome in asymptomatic patients with AS. One such trial that has recently commenced is Early Valve Replacement Guided by Biomarkers of LV Decompensation in Asymptomatic Patients with Severe AS (EVOLVED-AS); NCT03094143, which randomises patients with CMRI-detected fibrosis to surgery versus a watchful waiting approach.

T1 mapping

LGE detects focal areas of scarring. It cannot quantify interstitial/diffuse fibrosis. Interstitial fibrosis is associated with increased collagen content and increased myocardial

Figure 5 TAVI implant sizing. (1) 3D respiratory-gated bSSFP mages acquired in coronal view. (2) Post-processing reconstructed images from 3D bSSFP to determine the right and left ostail coronary artery height (14 and 12 mm, respectively). (3) Aortic root, sinuses and proximal course of the coronary arteries. (4) The cross-section of LVOT planimetry.

Please cite this article as: Mahon C, Mohiaddin RH, The emerging applications of cardiovascular magnetic resonance imaging in transcatheter aortic valve implantation, Clinical Radiology, https://doi.org/10.1016/j.crad.2019.11.011

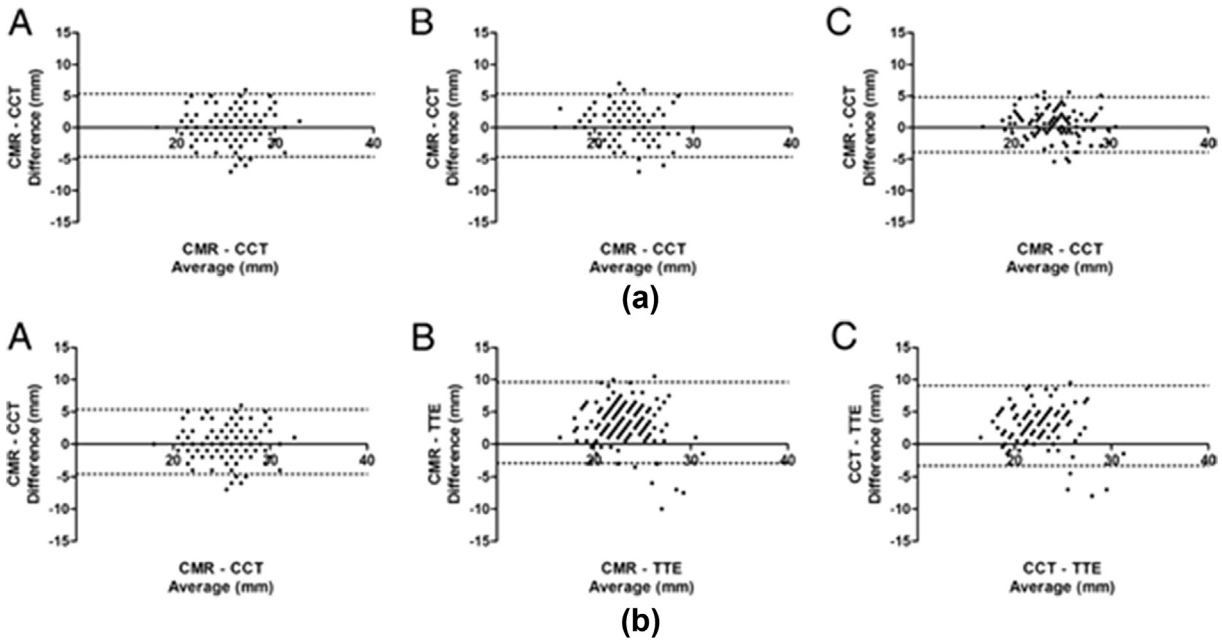

Figure 6 (a) Bland–Altman plots demonstrating close agreement between cardiovascular magnetic resonance (CMR)- and cardiac computed tomography (CCT)-derived aortic valve annulus diameters. (1) The largest annulus diameter, (2) smallest annulus diameter, and (3) average annulus diameter show similar agreements. Upper and lower dotted lines demote the 95% limits of agreement; the middle solid line is the bias. (b) Bland–Altman plots demonstrating closer agreement and lower bias for (1) CMRI- and cardiac CT (CCT)-derived aortic valve annulus diameters compared with (2) combined CMRI–TTE and (3) combined CMRI–CCT. Upper and lower dotted lines demote the 95% limits of agreement; the middle solid line is the bias. (Reproduced with permission from Jabbour A, Ismail TF, Moat N *et al.* Multimodality imaging in transcatheter aortic valve implantation and post-procedural aortic regurgitation: comparison among cardiovascular magnetic resonance, cardiac computed tomography, and echocardiography. J Am Coll Cardiol. 2011 Nov 15; 58:2165-73.)

extracellular volume fraction (ECV). T1 mapping directly measures the T1 relaxation time of the myocardium pre- and post-contrast. The change of the T1 relaxation rate in blood between pre-and post-contrast imaging is converted with the blood haematocrit into a reference for plasma T1, which serves as reference for the T1 changes in tissue.[71] This allows calculation of ECV, which is a surrogate of diffuse interstitial fibrosis.[50,72] In this method all the ECV, including the normal matrix supporting myocytes, intramyocardial blood vessels, and diffuse interstitial fibrosis are measured.[73] ECV can therefore be confounded by other parameters such as haemoglobin. The haematocrit is therefore required for accurate calculation of the ECV. There are characteristic T1 relaxation times for tissues at selected magnetic field strength that depends on tissue composition and therefore deviation from normal ranges can be used to detect and quantify pathological processes.[50] The MOLLI sequence is used to quantify T1. It is based on the earlier look-locker (LL) sequence consisting of a gradient echo sequence with a non-slice selective inversion pulse after an R wave followed by a segmented gradient echo acquisition applied both pre- and post-contrast medium.[18,68,69] The MOLLI sequence merges three successive ECG-triggered LL experiments carried out with three, three, and five single-shot readouts, respectively. Undisturbed magnetisation recovery is allowed between each LL experiment, with variation based on heart rate, and the reconstruction and preparation time of the CMR.[74] Subsequent images are acquired at time trigger delay after every R-wave, until the final number of images for each LL experiment is acquired. A shortened MOLLI sequence has also been recently tested.[75] This uses sequential inversion recovery measurements within a single breath-hold.

Native T1 values have been shown to be higher in patients with severe symptomatic AS compared with age-matched controls and are moderately correlated with fibrosis on histology[76]; however, no differences in either T1 or ECV were found between asymptomatic patients with moderate to severe AS and age-matched controls, suggesting its limited role in assessing individual patients.[54]

T1 mapping has been correlated with histological diffuse myocardial fibrosis,[77] and been used to track LV mass regression post-AVR, which comprises a combination of cellular and matrix volume reduction, demonstrating cellular regression, and no change in focal fibrosis (LGE).[78] It, therefore, holds promise as an important imaging marker of disease progression in AS, and may provide an ideal tool in the future in timing of intervention and as endpoints in therapeutic trials of anti-fibrotic agents.

Amyloidosis is caused by deposition of abnormally folded protein resulting in progressive organ dysfunction. It has been demonstrated that one in seven patients currently undergoing TAVR have occult amyloidosis.[79] The confirmation of such a high prevalence of occult amyloid in TAVI

Please cite this article as: Mahon C, Mohiaddin RH, The emerging applications of cardiovascular magnetic resonance imaging in transcatheter aortic valve implantation, Clinical Radiology, https://doi.org/10.1016/j.crad.2019.11.011

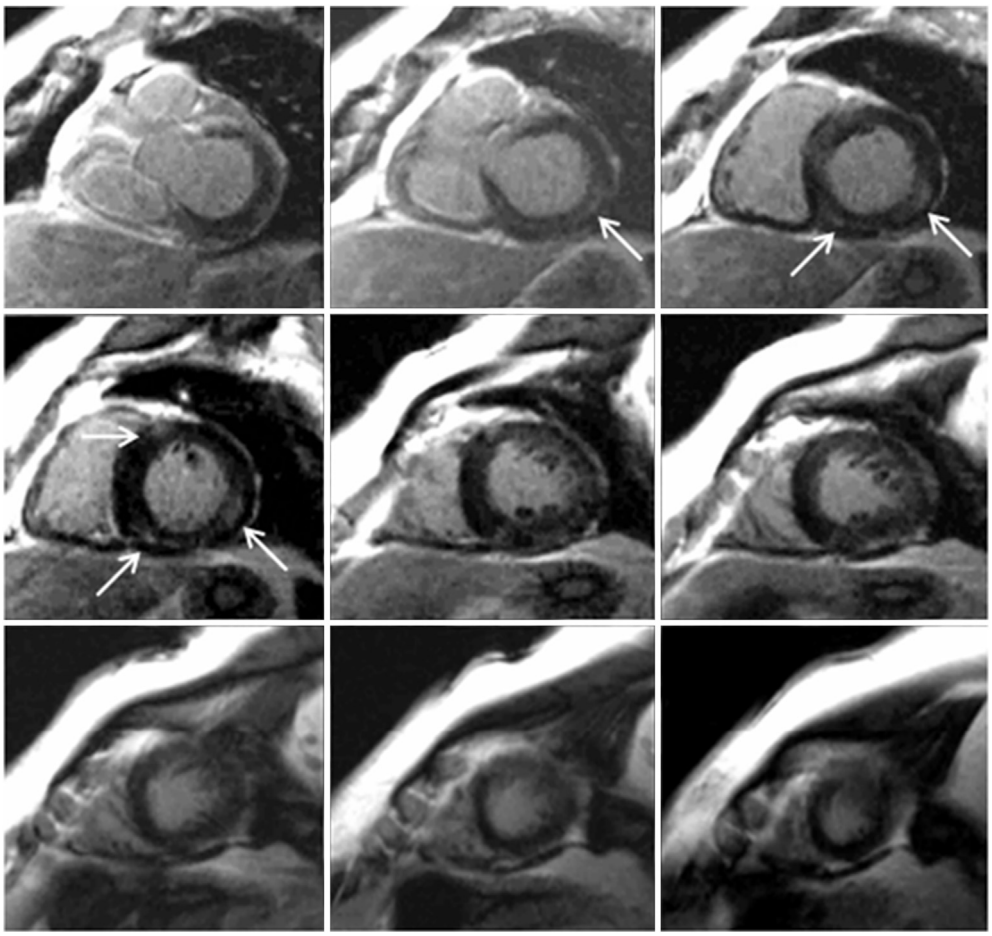

Figure 7 LGE images in the short axis view of the LV from base to apex showing focal mid-wall myocardial fibrosis in a patient with long-standing severe AS. The arrows show an area of intramyocardial LGE in the basal and mid-inferolateral and inferior wall.

patients has implications, placing these patients at higher risk for procedural success and outcome. The importance of this finding is still ongoing. Previously amyloid was a diagnosis driven by invasive cardiac biopsy. CMRI can non-invasively detect amyloid using assessment of hypertrophy, pericardial effusion, pre- and post-T1 mapping and LGE.[80] In cardiac amyloidosis, CMRI shows characteristic high myocardial gadolinium concentrations early after injection, and global subendocardial LGE is common. In addition, there are distinctively elevated pre- and post-T1 mapping values (using ECV as described above).[79] These findings have diagnostic valve and may prove useful in the quantitative evaluation of the change in myocardial amyloid burden with new treatments.[81] An example of elevated native myocardial T1 mapping as seen in amyloid is seen in Fig 8.

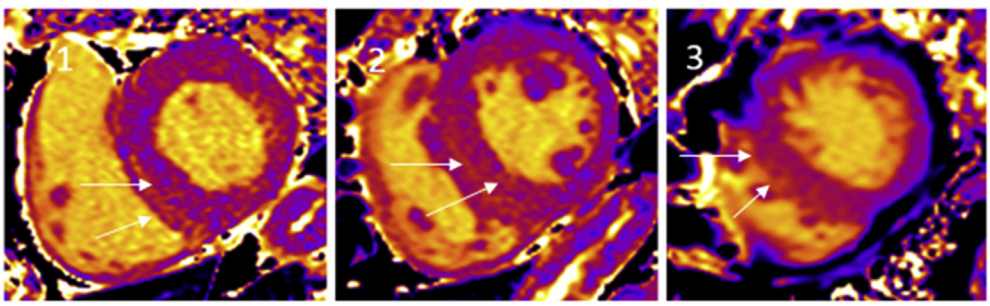

Figure 8 T1 myocardial mapping in the basal, mid and apical myocardial segments in patients with severe aortic valve stenosis. (1) Native myocardial T1 values is elevated in the basal septal and lateral wall. (2) Elevated native myocardial T1 values (1,142 ms at 1.5 T) in the mid septal wall. (3) Elevated T1 values in the apical septal wall (1,137 ms at 1.5 T).

Please cite this article as: Mahon C, Mohiaddin RH, The emerging applications of cardiovascular magnetic resonance imaging in transcatheter aortic valve implantation, Clinical Radiology, https://doi.org/10.1016/j.crad.2019.11.011

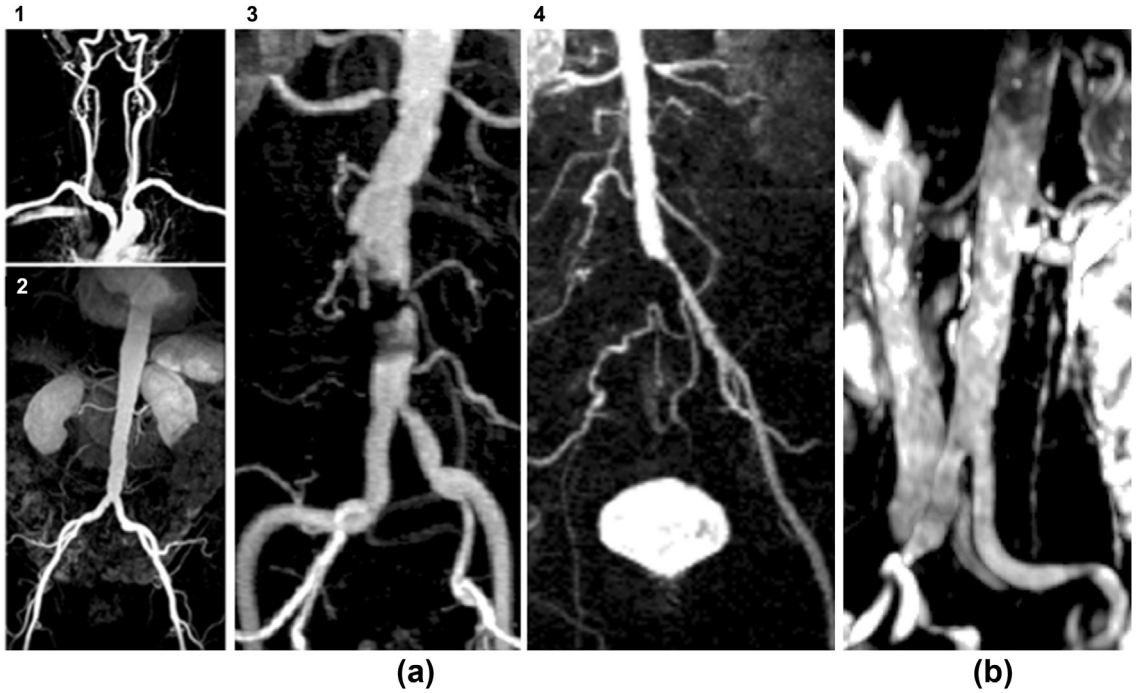

Figure 9 (a) (1) Maximum intensity projection images (MIP) contrast-enhanced magnetic resonance angiography (MRA) of the subclavian arteries (1) and the iliofemoral arteries and abdominal aorta (2) with minor vascular disease. Both routes are suitable for the TAVI procedure. (3) Maximum intensity projection images (MIP) contrast-enhanced image in the coronal view demonstrating a large partially thrombosed calcified aortic plaque almost obstructing aortic lumen at this level and precluding vascular access for TAVI via this route. There is also severe stenosis of the origin of the left common iliac artery and bilateral renal artery stenosis. (4) MIP contrast-enhanced MRA in coronal view of iliofemoral arteries with right iliac obstruction and left renal artery stenosis precluding vascular access for TAVI via this route. (b) Non-contrast MRA of the abdominal aorta and iliac arteries. Targeted MIP reconstructed from respiratory-gated 3D SSFP in coronal view. The iliac arteries are tortuous with focal bilateral stenoses. Note that in this type of angiography, the veins and some soft tissues return high signal as well.

Aorta and peripheral vasculature imaging

CMRI allows for a comprehensive assessment of the aorta and peripheral vasculature. It identifies atheromatous plaques and complex anatomy, such as aneurysm, dissection, intramural haematoma, and congenital abnormalities. It can provide a virtual roadmap in the pre-TAVI planning. This roadmap helps decisions regarding access sites, determine ostial height, annular dimensions, LVOT dimensions, and anticipate complications (Fig 9). The main limitation of CMRI assessment of vasculature is determining calcification, a common finding in the elderly.

The imaging protocol of the aorta involves a combination of multi-slice bSSFP imaging and HASTE pilot images acquired in sagittal, transaxial, and coronal in diastole and during a breath-hold gradient echo pulse sequences can be used if there is significant turbulent flow or valve-related metal artefact. The oblique sagittal cine is obtained by aligning the sequence orthogonal to the coronal scout in the axis of the LVOT and proximal ascending aorta. An oblique coronal acquisition is then located orthogonal to the oblique sagittal cine (LVOT cross-cut) aligned with the axis of the LVOT. The aortic annulus is measured from LVOT and LVOT cross cut. All aortic measurements are made using the 70–80% cardiac phase (R–R interval) cine images in end-diastole. The internal aorta dimensions are measured as the largest diameter and at 90° to this line measured. Peripheral vascular imaging use 3D contrast-enhanced MRA or 3D bSSFP without contrast medium administration.

CMRI can also provide insights into the mechanisms involved in aortopathy and non-invasive measures of aortic stiffness. With 4D flow imaging, a more detailed assessment of flow patterns and wall shear stress can be imaged. This technique has demonstrated differences in systolic flow patterns between bicuspid and tricuspid valves and the BAV subtypes[82,83] with right-handed helical flow and right-anterior flow jets in type-I BAV and left-handed helical flow with left-posterior flow jets in type-II BAV.[52]

Real-time CMRI-guided TAVI

TAVI has been successfully implanted in animal models using custom-engineered delivery systems with non-ferromagnetic materials[84,85]; however, at present, real-time CMRI-guided TAVI in humans is not possible. The potential for a non-nephrotoxic contrast TAVI procedure is attractive for patients with renal failure; however, it is unclear whether the improved soft-tissue visualisation and lack of ionising radiation confer a genuine benefit over X-ray fluoroscopy and echocardiography for TAVI. At present, there are no stiff interventional guidewires or MRI conditional temporary wires commercially available. Moreover,

Please cite this article as: Mahon C, Mohiaddin RH, The emerging applications of cardiovascular magnetic resonance imaging in transcatheter aortic valve implantation, Clinical Radiology, https://doi.org/10.1016/j.crad.2019.11.011

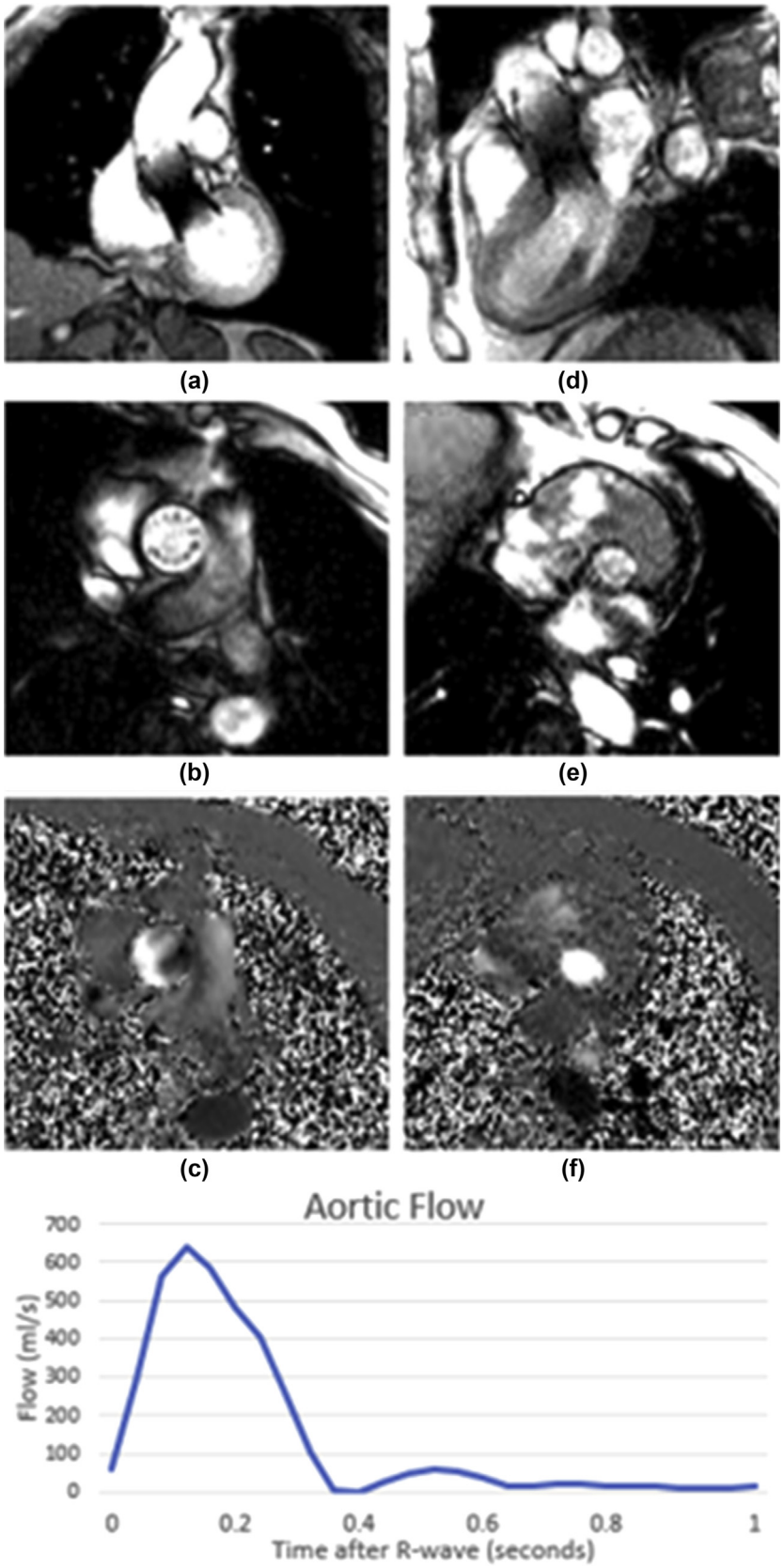

Figure 10 Corevalve (MedtronicTM) post-TAVI CMR. (a,b) Gradient echo images in two LVOT views showing in situ Corevalve-related metal artefact. (c) Gradient echo images immediately above and (d) immediately below the Corevalve with the corresponding systolic frame of flow mapping (e,f). (e) Flow volume curve above or below the valve showing no regurgitation.

Please cite this article as: Mahon C, Mohiaddin RH, The emerging applications of cardiovascular magnetic resonance imaging in transcatheter aortic valve implantation, Clinical Radiology, https://doi.org/10.1016/j.crad.2019.11.011

managing complications in the MRI environment offers logistical problems likely requiring evacuation of the patient from the MRI room to allow non-MRI compatible equipment to be used.

Post-TAVI

The TAVI implant is CMRI compatible and produces minimal artefact from the nitinol/cobalt chromium frame. Therefore, in the absence of contraindication to CMR, TAVI patients can be safely followed-up with CMRI (Fig 10). The stability and function of the prosthetic valve has important clinical impact on post-TAVI outcome and can be monitored and assessed by CMR. This is particularly relevant for assessment of paravalvular regurgitation (PAR), which can be difficult to assess with TTE, thrombus assessment and LV remodelling post-TAVI as previously discussed. CMRI can detect left atrial appendage and aneurysmal thrombus; however, bioprosthetic valve thrombosis can be difficult to detect with CMRI due to the fast motion of the thrombus.[3] The temporal and spatial resolution of CMRI may not be high enough to detect visually in cases of small thrombi, albeit increases in bioprosthetic valve gradient post TAVI can act as a surrogate marker to thrombus.

Paravalvular leak

The occurrence of residual PAR remains a major limitation of the TAVI procedure.[86,87] Moderate to severe PAR has been associated with increased short-term and long-term mortality following TAVI, and even mild PAR have been linked to poorer outcomes.[88,89] Therefore, an accurate assessment of post-TAVI PAR is of major prognostic importance.

Echocardiography, aortic root angiography, and haemodynamics are commonly used to assess the severity of PAR immediately post-TAVI; however, if PAR assessment is performed while the patient remains under sedation the effect of a low blood pressure may artificially underestimate the value. Therefore, a more accurate assessment of PAR typically relies on a post-procedural TTE.

CMRI can quantify PAR. CMRI uses the PC velocity mapping technique to assess PAR. If significant turbulence, aliasing or prosthesis stent-related artefacts are seen the acquisition is repeated a few millimetres downstream from the valve and/or with a higher-velocity window.[90] Importantly, CMRI has proven superior to echocardiography with both balloon-expandable and self-expandable implants.[64,90,91] Compared with qualitative echocardiography, CMRI reclassified at least one grade higher in almost 50% of patients.[92,93]

MRI and cerebral hits

Neurological complications in the setting of TAVI remain a concern, especially with the expansion of the technique toward younger patients. Most of the cerebrovascular events post-TAVI are embolic in origin, with <5% reported as haemorrhagic strokes.[94] Cerebrovascular complications related to TAVI demonstrate a significant variability between centres and studies, ranging from 1 to 11%.[95] This variability is in part explained by study design, diagnostic methods, patient risk profile, patient-specific factors, and systematic evaluation by a neurologist.[96–98] Diffusion-weighted MRI (DWI) of the brain is the technique of choice to identify cerebral embolic events. Studies with DWI demonstrate that between 60 and 90% of patients have new silent cerebral lesions after TAVI, independently of the vascular access or implant type.[99–102] Improvement in implant performance, procedural techniques, antithrombotic therapy and operator experience can lead to a significant reduction in the amount of cardio-embolic complications. Embolic protection devices have emerged as a potential solution to decrease cerebral embolisation and the associated neurological effects. To date, four embolic protection devices have been studied, with differences mainly in terms of design and access routes. Current study data indicate that embolic protection device use during TAVI reduced the risk of silent cerebrovascular infarction; however, results of ongoing larger clinical trials are pending.[103]

Conclusion

Cardiac imaging plays an essential role in selecting anatomical suitability for TAVI. CMRI has been underutilised in patient selection and follow-up, in favour of faster, and more widely available techniques such as TTE and MDCT. CMRI plays a role in patients with poor echocardiographic images, with renal dysfunction, contraindications to iodinated contrast agents, or when there is disparity between the findings of other techniques and/or clinical assessment; however, the use of CMRI in patients undergoing or being considered for TAVI is likely to expand with the availability of faster imaging techniques on modern CMRI systems and the expansion of TAVI clinical indications. With the ever-evolving role of TAVI in intermediate-risk patients, failing prosthetic valves, native aortic regurgitation, and younger patients with bicuspid aortic valves and complex anatomy, a radiation free method of assessment requiring no nephrotoxic contrast agent is highly attractive.

CMRI can provide important structural and functional information comparable to that obtained by both echocardiography and MDCT in patients under consideration for TAVI. As mentioned earlier, CMRI has limitations including assessment of calcification, cost, and availability in many healthcare settings. It provides accurate assessment of AS severity. The pathophysiological consequences of AS can be assessed, including the effects on ventricular volumes, function, mass, and myocardium characterisation. Several measurements can be obtained with high reproducibility and accuracy including the AV annulus, sinus, ostial height, aortic, and access routes dimensions. Its accuracy in these measurements, in terms of predicting the presence and severity of PAR after TAVI, are comparable with those obtained using CT. In the post-TAVI follow-up assessment,

Please cite this article as: Mahon C, Mohiaddin RH, The emerging applications of cardiovascular magnetic resonance imaging in transcatheter aortic valve implantation, Clinical Radiology, https://doi.org/10.1016/j.crad.2019.11.011

CMRI can detect and quantify paravalvular leaks and LV remodelling in a superior fashion to TTE. As discussed in the body of the text, there is unique opportunity for CMRI to provide an imaging biomarkers tool for AS risk-stratification. In the long-term, a role may arise for interventional CMRI for percutaneous valve interventions guidance such as TAVI. Finally, unnecessary duplication of imaging techniques should be avoided to reduce healthcare cost and to minimise inconvenience to patients. Ultimately, unless CMRI can be shown to lead to safer and better specific clinical outcome for patients under consideration for TAVI, the time and expense to preform CMRI on a routine basis will remain debatable.

Conflicts of interest

The authors declare no conflict of interest.

References

1. Keogh BB, Kinsman R, Walton P. *Demonstrating quality: the sixth national adult cardiac surgery database report*. Henley upon Thames: Dendrite Clinical Systems Ltd; 2009.
2. Lindroos M, Kupari M, Heikkilä J, *et al*. Prevalence of aortic valve abnormalities in the elderly: an echocardiographic study of a random population sample. *J Am Coll Cardiol* 1993;**21**(5):1220–5. https://doi.org/10.1016/0735-1097(93)90249-Z.
3. Baumgartner H, Falk V, Bax JJ, *et al*. 2017 ESC/EACTS guidelines for the management of valvular heart disease. *Eur Heart J* 2017;**38**(36):2739–91. https://doi.org/10.1093/eurheartj/ehx391.
4. Smith CR, Leon MB, Mack MJ, *et al*. Transcatheter versus surgical aortic-valve replacement in high-risk patients. *N Engl J Med* 2011;**364**(23):2187–98. https://doi.org/10.1056/NEJMoa1103510.
5. Reardon MJ, Adams DH, Kleiman NS, *et al*. 2-Year outcomes in patients undergoing surgical or self-expanding transcatheter aortic valve replacement. *J Am Coll Cardiol* 2015;**66**(2):113–21. https://doi.org/10.1016/j.jacc.2015.05.017.
6. Leon MB, Smith CR, Mack MJ, *et al*. Transcatheter or surgical aortic-valve replacement in intermediate-risk patients. *N Engl J Med* 2016;**374**(17):1609–20. https://doi.org/10.1056/NEJMoa1514616.
7. Arias EA, Bhan A, Lim ZY, *et al*. TAVI for pure native aortic regurgitation: are we there yet? *Interv Cardiol (London, England)* 2019;**14**(1):26–30. https://doi.org/10.15420/icr.2018.37.1.
8. Ribeiro HB, Webb JG, Makkar RR, *et al*. Predictive factors, management, and clinical outcomes of coronary obstruction following transcatheter aortic valve implantation: insights from a large multicenter registry. *J Am Coll Cardiol* 2013;**62**(17):1552–62. https://doi.org/10.1016/j.jacc.2013.07.040.
9. Bleakley C, Monaghan MJ. The pivotal role of imaging in TAVR procedures. *Curr Cardiol Rep* 2018;**20**(2):9. https://doi.org/10.1007/s11886-018-0949-z.
10. Onishi T, Sengoku K, Ichibori Y, *et al*. The role of echocardiography in transcatheter aortic valve implantation. *Cardiovasc Diagn Ther* 2018;**8**(1):3–17. https://doi.org/10.21037/cdt.2018.01.06.
11. Auffret V, Lefevre T, Van Belle E, *et al*. Temporal trends in transcatheter aortic valve replacement in France: France 2 to France TAVI. *J Am Coll Cardiol* 2017;**70**(1):42–55. https://doi.org/10.1016/j.jacc.2017.04.053.
12. Achenbach S, Delgado V, Hausleiter J, *et al*. SCCT expert consensus document on computed tomography imaging before transcatheter aortic valve implantation (TAVI)/transcatheter aortic valve replacement (TAVR). *J Cardiovasc Comput Tomogr* 2012;**6**(6):366–80. https://doi.org/10.1016/j.jcct.2012.11.002.
13. Kerner A, Abadi S, Dotan R, *et al*. Automatic estimation of optimal deployment of transcatheter aortic valve implantation using computed tomography. *J Heart Valve Dis* 2017;**26**:130–8.
14. Bloomfield GS, Gillam LD, Hahn RT, *et al*. A practical guide to multimodality imaging of transcatheter aortic valve replacement. *JACC Cardiovasc Imaging* 2012;**5**(4):441–55. https://doi.org/10.1016/j.jcmg.2011.12.013.
15. Bottini PB, Carr AA, Prisant LM, *et al*. Magnetic resonance imaging compared to echocardiography to assess left ventricular mass in the hypertensive patient. *Am J Hypertens* 1995;**8**(3):221–8. https://doi.org/10.1016/0895-7061(94)00178-E.
16. Grothues F, Smith GC, Moon JCC, *et al*. Comparison of interstudy reproducibility of cardiovascular magnetic resonance with two-dimensional echocardiography in normal subjects and in patients with heart failure or left ventricular hypertrophy. *Am J Cardiol* 2002;**90**(1):29–34. https://doi.org/10.1016/S0002-9149(02)02381-0.
17. Nishimura RA, Otto Cm, RO Bonow, *et al*. 2017 AHA/ACC focused update of the 2014 AHA/ACC guideline for the management of patients with valvular heart disease: a report of the American College of Cardiology/American Heart Association Task Force on clinical practice guidelines. *Circulation* 2017;**135**(25):e1159–95. https://doi.org/10.1161/CIR.0000000000000503.
18. Azevedo CF, Nigri M, Higuchi ML, *et al*. Prognostic significance of myocardial fibrosis quantification by histopathology and magnetic resonance imaging in patients with severe aortic valve disease. *J Am Coll Cardiol* 2010;**56**(4):278–87. https://doi.org/10.1016/j.jacc.2009.12.074.
19. Singh A, McCann GP. Cardiac magnetic resonance imaging for the assessment of aortic stenosis. *Heart* 2019;**105**(6):489–97. https://doi.org/10.1136/heartjnl-2018-313003.
20. Pontone G, Andreini D, Bartorelli AL, *et al*. Comparison of accuracy of aortic root annulus assessment with cardiac magnetic resonance versus echocardiography and multidetector computed tomography in patients referred for transcatheter aortic valve implantation. *Am J Cardiol* 2013;**112**(11):1790–9. https://doi.org/10.1016/j.amjcard.2013.07.050.
21. Suchá D, Tuncay V, Prakken NHJ, *et al*. Does the aortic annulus undergo conformational change throughout the cardiac cycle? A systematic review. *Eur Hear J Cardiovasc Imaging* 2015;**16**(12):1307–17. https://doi.org/10.1093/ehjci/jev210.
22. Francone M, Budde RPJ, Bremerich J, *et al*. CT and MR imaging prior to transcatheter aortic valve implantation: standardisation of scanning protocols, measurements and reporting—a consensus document by the European Society of Cardiovascular Radiology (ESCR). *Eur Radiol* 2019, https://doi.org/10.1007/s00330-019-06357-8.
23. Zamorano JL, Gonçalves A, Lang R. Imaging to select and guide transcatheter aortic valve implantation. *Eur Heart J* 2014;**35**(24):1578–87. https://doi.org/10.1093/eurheartj/eht569.
24. Alfudhili K, Masci PG, Delacoste J, *et al*. Current artefacts in cardiac and chest magnetic resonance imaging: tips and tricks. *Br J Radiol* 2016;**89**(1062), https://doi.org/10.1259/bjr.20150987.
25. Maeno Y, Abramowitz Y, Kawamori H, *et al*. A highly predictive risk model for pacemaker implantation after TAVR. *JACC Cardiovasc Imaging* 2017;**10**(10, Part A):1139–47. https://doi.org/10.1016/j.jcmg.2016.11.020.
26. Terré JA, George I, Smith CR. Pros and cons of transcatheter aortic valve implantation (TAVI). *Ann Cardiothorac Surg* 2017;**6**(5):444–52. https://doi.org/10.21037/acs.2017.09.15.
27. O'Brien KR, Cowan BR, Jain M, *et al*. MRI phase contrast velocity and flow errors in turbulent stenotic jets. *J Magn Reson Imaging* 2008;**28**(1):210–8. https://doi.org/10.1002/jmri.21395.
28. CS D, Jiuan LS, Peggy B, *et al*. Practical value of cardiac magnetic resonance imaging for clinical quantification of aortic valve stenosis. *Circulation* 2003;**108**(18):2236–43. https://doi.org/10.1161/01.CIR.0000095268.47282.A1.
29. Marckmann P, Skov L, Rossen K, *et al*. Nephrogenic systemic fibrosis: suspected causative role of gadodiamide used for contrast-enhanced magnetic resonance imaging. *J Am Soc Nephrol* 2006;**17**(9):2359–62. https://doi.org/10.1681/ASN.2006060601.
30. Bennett CL, Qureshi ZP, Sartor AO, *et al*. Gadolinium-induced nephrogenic systemic fibrosis: the rise and fall of an iatrogenic disease. *Clin Kidney J* 2012;**5**(1):82–8. https://doi.org/10.1093/ckj/sfr172.
31. Kanda T, Ishii K, Kawaguchi H, *et al*. High signal intensity in the dentate nucleus and globus pallidus on unenhanced T1-weighted MR images: relationship with increasing cumulative dose of a gadolinium-based

Please cite this article as: Mahon C, Mohiaddin RH, The emerging applications of cardiovascular magnetic resonance imaging in transcatheter aortic valve implantation, Clinical Radiology, https://doi.org/10.1016/j.crad.2019.11.011

contrast material. *Radiology* 2013;**270**(3):834–41. https://doi.org/10.1148/radiol.13131669.
32. Errante Y, Cirimele V, Mallio CA, *et al.* Progressive increase of T1 signal intensity of the dentate nucleus on unenhanced magnetic resonance images is associated with cumulative doses of intravenously administered gadodiamide in patients with normal renal function, suggesting dechelation. *Invest Radiol* 2014;**49**(10).
33. Bellenger NG, Davies LC, Francis JM, *et al.* Reduction in sample size for studies of remodeling in heart failure by the use of cardiovascular magnetic resonance. *J Cardiovasc Magn Reson* 2000;**2**(4):271–8. https://doi.org/10.3109/10976640009148691.
34. Maceira AM, Prasad SK, Khan M, *et al.* Normalized left ventricular systolic and diastolic function by steady state free precession cardiovascular magnetic resonance. *J Cardiovasc Magn Reson* 2006;**8**(3):417–26. https://doi.org/10.1080/10976640600572889.
35. Dweck MR, Joshi S, Murigu T, *et al.* Left ventricular remodeling and hypertrophy in patients with aortic stenosis: insights from cardiovascular magnetic resonance. *J Cardiovasc Magn Reson* 2012;**14**(1):50. https://doi.org/10.1186/1532-429X-14-50.
36. Lee VS, Resnick D, Bundy JM, *et al.* Cardiac function: MR evaluation in one breath hold with real-time true fast imaging with steady-state precession. *Radiology* 2002;**222**(3):835–42. https://doi.org/10.1148/radiol.2223011156.
37. Kaplan W. *Advanced calculus*. New York: Addison-Wesley; 2002.
38. Strohm O, Schulz-Menger J, Pilz B, *et al.* Measurement of left ventricular dimensions and function in patients with dilated cardiomyopathy. *J Magn Reson Imaging* 2001;**13**(3):367–71. https://doi.org/10.1002/jmri.1052.
39. Cerqueira Manuel D, Weissman Neil J, Vasken D, *et al.* Standardized myocardial segmentation and nomenclature for tomographic imaging of the heart. *Circulation* 2002;**105**(4):539–42. https://doi.org/10.1161/hc0402.102975.
40. Levy D, Garrison RJ, Savage DD, *et al.* Prognostic implications of echocardiographically determined left ventricular mass in the Framingham Heart Study. *N Engl J Med* 1990;**322**(22):1561–6. https://doi.org/10.1056/NEJM199005313222203.
41. Ghali JK, Liao Y, Simmons B, *et al.* The prognostic role of left ventricular hypertrophy in patients with or without coronary artery disease. *Ann Intern Med* 1992;**117**(10):831–6. https://doi.org/10.7326/0003-4819-117-10-831.
42. Sokolow M, Lyon TP. The ventricular complex in left ventricular hypertrophy as obtained by unipolar precordial and limb leads. *Am Heart J* 1949;**37**(2):161–86. https://doi.org/10.1016/0002-8703(49)90562-1.
43. Romhilt DW, Estes EH. A point-score system for the ECG diagnosis of left ventricular hypertrophy. *Am Heart J* 1968;**75**(6):752–8. https://doi.org/10.1016/0002-8703(68)90035-5.
44. Woythaler JN, Singer SL, Kwan OL, *et al.* Accuracy of echocardiography versus electrocardiography in detecting left ventricular hypertrophy: comparison with postmortem mass measurements. *J Am Coll Cardiol* 1983;**2**(2):305–11. https://doi.org/10.1016/S0735-1097(83)80167-3.
45. Khaled A, Kevin W, Tim J, *et al.* New gender-specific partition values for ECG criteria of left ventricular hypertrophy. *Hypertension* 2004;**44**(2):175–9. https://doi.org/10.1161/01.HYP.0000135249.66192.30.
46. Maron MS, Maron BJ, Harrigan C, *et al.* Hypertrophic cardiomyopathy phenotype revisited after 50 years with cardiovascular magnetic resonance. *J Am Coll Cardiol* 2009;**54**(3):220–8. https://doi.org/10.1016/j.jacc.2009.05.006.
47. Katz J, Milliken MC, Stray-Gundersen J, *et al.* Estimation of human myocardial mass with MR imaging. *Radiology* 1988;**169**(2):495–8. https://doi.org/10.1148/radiology.169.2.2971985.
48. Khouri MG, Peshock RM, Ayers CR, *et al.* A 4-tiered classification of left ventricular hypertrophy based on left ventricular geometry. *Circ Cardiovasc Imaging* 2010;**3**(2):164–71. https://doi.org/10.1161/CIRCIMAGING.109.883652.
49. Fox ER, Taylor J, Taylor H, *et al.* Left ventricular geometric patterns in the Jackson cohort of the atherosclerotic risk in communities (ARIC) study: clinical correlates and influences on systolic and diastolic dysfunction. *Am Heart J* 2007;**153**(2):238–44. https://doi.org/10.1016/j.ahj.2006.09.013.
50. Maceira AM, Mohiaddin RH. Cardiovascular magnetic resonance in systemic hypertension. *J Cardiovasc Magn Reson* 2012;**14**(1):28. https://doi.org/10.1186/1532-429X-14-28.
51. Lorenza MM, Massimo S, Cristina M, *et al.* Left ventricular concentric geometry during treatment adversely affects cardiovascular prognosis in hypertensive patients. *Hypertension* 2004;**43**(4):731–8. https://doi.org/10.1161/01.HYP.0000121223.44837.de.
52. Pennell DJ, Sechtem UP, Higgins CB, *et al.* Clinical indications for cardiovascular magnetic resonance (CMR): consensus panel report. *Eur Heart J* 2004;**25**(21):1940–65. https://doi.org/10.1016/j.ehj.2004.06.040.
53. Fairbairn TA, Steadman CD, Mather AN, *et al.* Assessment of valve haemodynamics, reverse ventricular remodelling and myocardial fibrosis following transcatheter aortic valve implantation compared to surgical aortic valve replacement: a cardiovascular magnetic resonance study. *Heart* 2013;**99**(16):1185–91. https://doi.org/10.1136/heartjnl-2013-303927.
54. Singh A, Horsfield MA, Bekele S, *et al.* Myocardial T1 and extracellular volume fraction measurement in asymptomatic patients with aortic stenosis: reproducibility and comparison with age-matched controls. *Eur Hear J Cardiovasc Imaging* 2015;**16**(7):763–70. https://doi.org/10.1093/ehjci/jev007.
55. Singh A, Chan DCS, Greenwood JP, *et al.* Symptom onset in aortic stenosis: relation to sex differences in left ventricular remodeling. *JACC Cardiovasc Imaging* 2019;**12**(1):96–105. https://doi.org/10.1016/j.jcmg.2017.09.019.
56. Kupfahl C, Honold M, Meinhardt G, *et al.* Evaluation of aortic stenosis by cardiovascular magnetic resonance imaging: comparison with established routine clinical techniques. *Heart* 2004;**90**(8):893–901. https://doi.org/10.1136/hrt.2003.022376.
57. John AS, Dill T, Brandt RR, *et al.* Magnetic resonance to assess the aortic valve area in aortic stenosis: how does it compare to current diagnostic standards? *J Am Coll Cardiol* 2003;**42**(3):519–26. https://doi.org/10.1016/S0735-1097(03)00707-1.
58. Clavel M-A, Malouf J, Messika-Zeitoun D, *et al.* Aortic valve area calculation in aortic stenosis by CT and Doppler echocardiography. *JACC Cardiovasc Imaging* 2015;**8**(3):248–57. https://doi.org/10.1016/j.jcmg.2015.01.009.
59. Tuncay V, Prakken N, van Ooijen PMA, *et al.* Semiautomatic, quantitative measurement of aortic valve area using CTA: validation and comparison with transthoracic echocardiography. *Biomed Res Int* 2015;**2015**:648283. https://doi.org/10.1155/2015/648283.
60. Manning WJ, Pennell DJ. *Cardiovascular magnetic resonance*. Saunders: Elsevier Health Sciences; 2010.
61. Kutty S, Whitehead KK, Natarajan S, *et al.* Qualitative echocardiographic assessment of aortic valve regurgitation with quantitative cardiac magnetic resonance: a comparative study. *Pediatr Cardiol* 2009;**30**(7):971–7. https://doi.org/10.1007/s00246-009-9490-6.
62. Mohiaddin RH, Longmore DB. Functional aspects of cardiovascular nuclear magnetic resonance imaging. Techniques and application. *Circulation* 1993;**88**(1):264–81. https://doi.org/10.1161/01.CIR.88.1.264.
63. Myerson SG. Heart valve disease: investigation by cardiovascular magnetic resonance. *J Cardiovasc Magn Reson* 2012;**14**(1):7. https://doi.org/10.1186/1532-429X-14-7.
64. Sherif M, Abdel-Wahab M, Beurich H-W, *et al.* Haemodynamic evaluation of aortic regurgitation after transcatheter aortic valve implantation using cardiovascular magnetic resonance. *EuroIntervention* 2011;**7**(1):57–63.
65. Gopal A, Grayburn PA, Mack M, *et al.* Noncontrast 3D CMRI imaging for aortic valve annulus sizing in TAVR. *JACC Cardiovasc Imaging* 2015;**8**(3):375–8. https://doi.org/10.1016/j.jcmg.2014.11.011.
66. Jabbour A, Ismail TF, Moat N, *et al.* Multimodality imaging in transcatheter aortic valve implantation and post-procedural aortic regurgitation: comparison among cardiovascular magnetic resonance, cardiac computed tomography, and echocardiography. *J Am Coll Cardiol* 2011;**58**(21):2165–73. https://doi.org/10.1016/j.jacc.2011.09.010.
67. Quail MA, Nordmeyer J, Schievano S, *et al.* Use of cardiovascular magnetic resonance imaging for TAVR assessment in patients with bioprosthetic aortic valves: comparison with computed tomography. *Eur J Radiol* 2012;**81**(12):3912–7. https://doi.org/10.1016/j.ejrad.2012.07.014.

Please cite this article as: Mahon C, Mohiaddin RH, The emerging applications of cardiovascular magnetic resonance imaging in transcatheter aortic valve implantation, Clinical Radiology, https://doi.org/10.1016/j.crad.2019.11.011

68. Flett AS, Hasleton J, Cook C, *et al.* Evaluation of techniques for the quantification of myocardial scar of differing etiology using cardiac magnetic resonance. *JACC Cardiovasc Imaging* 2011;**4**(2):150–6. https://doi.org/10.1016/j.jcmg.2010.11.015.
69. Frank W, Sebastian H, Stefan S, *et al.* Impact of myocardial fibrosis in patients with symptomatic severe aortic stenosis. *Circulation* 2009;**120**(7):577–84. https://doi.org/10.1161/CIRCULATIONAHA.108.847772.
70. Musa TA, Treibel TA, Vassiliou VS, *et al.* Myocardial scar and mortality in severe aortic stenosis. *Circulation* 2018;**138**(18):1935–47. https://doi.org/10.1161/CIRCULATIONAHA.117.032839.
71. Arheden H, Saeed M, Higgins CB, *et al.* Measurement of the distribution volume of gadopentetate dimeglumine at echo-planar MR imaging to quantify myocardial infarction: comparison with 99mTc-DTPA autoradiography in rats. *Radiology* 1999;**211**(3):698–708. https://doi.org/10.1148/radiology.211.3.r99jn41698.
72. Ugander M, Oki AJ, Hsu L-Y, *et al.* Extracellular volume imaging by magnetic resonance imaging provides insights into overt and subclinical myocardial pathology. *Eur Heart J* 2012;**33**(10):1268–78. https://doi.org/10.1093/eurheartj/ehr481.
73. Mahmod M, Piechnik SK, Levelt E, *et al.* Adenosine stress native T1 mapping in severe aortic stenosis: evidence for a role of the intravascular compartment on myocardial T1 values. *J Cardiovasc Magn Reson* 2014;**16**(1):92. https://doi.org/10.1186/s12968-014-0092-y.
74. Messroghli DR, Walters K, Plein S, *et al.* Myocardial T1 mapping: application to patients with acute and chronic myocardial infarction. *Magn Reson Med* 2007;**58**(1):34–40. https://doi.org/10.1002/mrm.21272.
75. White SK, Piechnik SK, Neubauer S, *et al.* Histological validation of ShMOLLI equilibrium contrast CMRI for the measurement of diffuse myocardial fibrosis. *J Cardiovasc Magn Reson* 2012;**14**(1):O111. https://doi.org/10.1186/1532-429X-14-S1-O111.
76. Bull S, White SK, Piechnik SK, *et al.* Human non-contrast T1 values and correlation with histology in diffuse fibrosis. *Heart* 2013;**99**(13):932–7. https://doi.org/10.1136/heartjnl-2012-303052.
77. Chin CWL, Everett RJ, Kwiecinski J, *et al.* Myocardial fibrosis and cardiac decompensation in aortic stenosis. *JACC Cardiovasc Imaging* 2017;**10**(11):1320–33. https://doi.org/10.1016/j.jcmg.2016.10.007.
78. Treibel TA, Kozor R, Schofield R, *et al.* Reverse myocardial remodeling following valve replacement in patients with aortic stenosis. *J Am Coll Cardiol* 2018;**71**(8):860–71. https://doi.org/10.1016/j.jacc.2017.12.035.
79. Castaño A, Narotsky DL, Hamid N, *et al.* Unveiling transthyretin cardiac amyloidosis and its predictors among elderly patients with severe aortic stenosis undergoing transcatheter aortic valve replacement. *Eur Heart J* 2017;**38**(38):2879–87. https://doi.org/10.1093/eurheartj/ehx350.
80. Cavalcante JL, Rijal S, Abdelkarim I, *et al.* Cardiac amyloidosis is prevalent in older patients with aortic stenosis and carries worse prognosis. *J Cardiovasc Magn Reson* 2017;**19**(1):98. https://doi.org/10.1186/s12968-017-0415-x.
81. Maria MA, Jayshree J, Kumar PS, *et al.* Cardiovascular magnetic resonance in cardiac amyloidosis. *Circulation* 2005;**111**(2):186–93. https://doi.org/10.1161/01.CIR.0000152819.97857.9D.
82. Meierhofer C, Schneider EP, Lyko C, *et al.* Wall shear stress and flow patterns in the ascending aorta in patients with bicuspid aortic valves differ significantly from tricuspid aortic valves: a prospective study. *Eur Hear J Cardiovasc Imaging* 2012;**14**(8):797–804. https://doi.org/10.1093/ehjci/jes273.
83. den Reijer PM, Sallee D 3rd, van der Velden P, *et al.* Hemodynamic predictors of aortic dilatation in bicuspid aortic valve by velocity-encoded cardiovascular magnetic resonance. *J Cardiovasc Magn Reson* 2010;**12**(1):4. https://doi.org/10.1186/1532-429X-12-4.
84. Horvath KA, Guttman M, Li M, *et al.* Beating heart aortic valve replacement using real-time MRI guidance. *Innovations* 2007;**2**(2):51–5. https://doi.org/10.1097/imi.0b013e31805b8280.
85. Kahlert P, Parohl N, Albert J, *et al.* Towards real-time cardiovascular magnetic resonance guided transarterial CoreValve implantation: in vivo evaluation in swine. *J Cardiovasc Magn Reson* 2012;**14**(1):21. https://doi.org/10.1186/1532-429X-14-21.
86. Généreux P, Head SJ, Hahn R, *et al.* Paravalvular leak after transcatheter aortic valve replacement: the new Achilles' heel? A comprehensive review of the literature. *J Am Coll Cardiol* 2013;**61**(11):1125–36. https://doi.org/10.1016/j.jacc.2012.08.1039.
87. Genereux P, Head SJ, Hahn R. Paravalvular aortic leak after transcatheter aortic valve replacement. *Circulation* 2013;**127**(3):397–407. https://doi.org/10.1161/CIRCULATIONAHA.112.142000.
88. Athappan G, Patvardhan E, Tuzcu EM, *et al.* Incidence, predictors, and outcomes of aortic regurgitation after transcatheter aortic valve replacement: meta-analysis and systematic review of literature. *J Am Coll Cardiol* 2013;**61**(15):1585–95. https://doi.org/10.1016/j.jacc.2013.01.047.
89. Kodali SK, Williams MR, Smith CR, *et al.* Two-year outcomes after transcatheter or surgical aortic-valve replacement. *N Engl J Med* 2012;**366**(18):1686–95. https://doi.org/10.1056/NEJMoa1200384.
90. Ribeiro HB, Le Ven F, Larose É, *et al.* Cardiac magnetic resonance versus transthoracic echocardiography for the assessment and quantification of aortic regurgitation in patients undergoing transcatheter aortic valve implantation. *Heart* 2014;**100**(24):1924–32. https://doi.org/10.1136/heartjnl-2014-305615.
91. Orwat S, Diller G-P, Kaleschke G, *et al.* Aortic regurgitation severity after transcatheter aortic valve implantation is underestimated by echocardiography compared with MRI. *Heart* 2014;**100**(24):1933–8. https://doi.org/10.1136/heartjnl-2014-305665.
92. Hartlage GR, Babaliaros VC, Thourani VH, *et al.* The role of cardiovascular magnetic resonance in stratifying paravalvular leak severity after transcatheter aortic valve replacement: an observational outcome study. *J Cardiovasc Magn Reson* 2014;**16**(1):93. https://doi.org/10.1186/s12968-014-0093-x.
93. Crouch G, Tully PJ, Bennetts J, *et al.* Quantitative assessment of paravalvular regurgitation following transcatheter aortic valve replacement. *J Cardiovasc Magn Reson* 2015;**17**(1):32. https://doi.org/10.1186/s12968-015-0134-0.
94. Miller DC, Blackstone EH, Mack MJ, *et al.* Transcatheter (TAVR) versus surgical (AVR) aortic valve replacement: occurrence, hazard, risk factors, and consequences of neurologic events in the PARTNER trial. *J Thorac Cardiovasc Surg* 2012;**143**(4):832–43. https://doi.org/10.1016/j.jtcvs.2012.01.055. e13.
95. Auffret V, Regueiro A, Del Trigo M, *et al.* Predictors of early cerebrovascular events in patients with aortic stenosis undergoing transcatheter aortic valve replacement. *J Am Coll Cardiol* 2016;**68**(7):673–84. https://doi.org/10.1016/j.jacc.2016.05.065.
96. Buellesfeld L, Wenaweser P, Gerckens U, *et al.* Transcatheter aortic valve implantation: predictors of procedural success—the Siegburg–Bern experience. *Eur Heart J* 2009;**31**(8):984–91. https://doi.org/10.1093/eurheartj/ehp570.
97. Stortecky S, Windecker S, Pilgrim T, *et al.* Cerebrovascular accidents complicating transcatheter aortic valve implantation: frequency, timing and impact on outcomes. *EuroIntervention* 2012;**8**(1):62–70.
98. Eltchaninoff H, Prat A, Gilard M, *et al.* Transcatheter aortic valve implantation: early results of the France (FRench Aortic National CoreValve and Edwards) registry. *Eur Heart J* 2010;**32**(2):191–7. https://doi.org/10.1093/eurheartj/ehq261.
99. Kahlert P, Knipp SC, Schlamann M, *et al.* Silent and apparent cerebral ischemia after percutaneous transfemoral aortic valve implantation. *Circulation* 2010;**121**(7):870–8. https://doi.org/10.1161/CIRCULATIONAHA.109.855866.
100. Arnold M, Schulz-Heise S, Achenbach S, *et al.* Embolic cerebral insults after transapical aortic valve implantation detected by magnetic resonance imaging. *JACC Cardiovasc Interv* 2010;**3**(11):1126–32. https://doi.org/10.1016/j.jcin.2010.09.008.
101. Ghanem A, Müller A, Nähle CP, *et al.* Risk and fate of cerebral embolism after transfemoral aortic valve implantation: a prospective pilot study with diffusion-weighted magnetic resonance imaging. *J Am Coll Cardiol* 2010;**55**(14):1427–32. https://doi.org/10.1016/j.jacc.2009.12.026.
102. Armijo G, Nombela-Franco L, Tirado-Conte G. Cerebrovascular events after transcatheter aortic valve implantation. *Front Cardiovasc Med* 2018;**5**:104.
103. Steinvil A, Benson RT, Waksman R. Contemporary reviews in interventional cardiology embolic protection devices in transcatheter aortic valve replacement. *Am Heart J* 2016;**9**(3):1–7. https://doi.org/10.1161/CIRCINTERVENTIONS.115.003284.

Please cite this article as: Mahon C, Mohiaddin RH, The emerging applications of cardiovascular magnetic resonance imaging in transcatheter aortic valve implantation, Clinical Radiology, https://doi.org/10.1016/j.crad.2019.11.011